ELSEVIER

Surface and Coatings Technology 115 (1999) 234–238

SURFACE & COATINGS TECHNOLOGY

www.elsevier.nl/locate/surfcoat

Improvement of tribological properties of 9Cr18 bearing steel using metal and nitrogen plasma-immersion ion implantation

Z.M. Zeng [a,b], T. Zhang [a], B.Y. Tang [a,b], X.B. Tian [a,b], P.K. Chu [a,*]

[a] *Department of Physics and Materials Science, City University of Hong Kong, 83 Tat Chee Avenue, Kowloon, Hong Kong*
[b] *Advanced Welding Production & Technology National Key Lab, Harbin Institute of Technology, Harbin, People's Republic of China*

Received 7 December 1998; accepted 24 April 1999

Abstract

Metal plasma-immersion ion implantation (PIII) employing an improved vacuum-arc plasma source is performed on 9Cr18 bearing steels. Titanium and tantalum ions are implanted followed by nitrogen plasma-immersion ion implantation to yield a modified surface layer with superior wear resistance. The surface properties of the 9Cr18 bearing steel samples are evaluated by measuring the microhardness, wear properties and coefficient of friction. Elemental depth profiles and the chemical composition of the modified layer are acquired by Auger electron spectroscopy and X-ray photoelectron spectroscopy. The results show that the wear resistance of the samples implanted with (Ti+N) and (Ta+N) is better than that of the samples undergoing nitrogen PIII alone. The XPS results indicate the presence of nitride phases in the implanted layer. In this paper, the new improvements made on the metal-arc source are described. Using the new procedures incorporating both metal-ion and gas PIII, the surface properties of 9Cr18 bearing steel are significantly improved.

Keywords: Bearing steel; Plasma-immersion ion implantation; Surface modification; Vacuum-arc plasma source

1. Introduction

Stainless steel bearings are widely used in industry. A failed bearing has a significant impact on a machine and the reliability of the whole system. Hence, prolonging the working lifetime and reliability of bearings can be beneficial especially in the aerospace and nuclear industry [1]. Previous studies have revealed that bearing failure occurs mainly on the surface or in the near-surface region [2]. Therefore, surface-modification techniques play an important role in the improvement of industrial bearings.

Plasma-immersion ion implantation (PIII) has no line-of-sight restriction and retained dose problem characteristic of conventional ion-beam implantation [3–6]. It is therefore an excellent surface-modification technique to treat complex-shaped industrial components such as precision bearings [7]. PIII also retains the advantages of beam-line ion implantation, e.g., the ability to introduce multiple elements at concentrations exceeding the solubility limits of conventional alloys [8]. Thus, implants of multiple species at high ion concentrations can produce alloys in the near-surface region.

Vacuum-arc plasma sources are based on vacuum-arc discharge between electrodes in a vacuum [9,10]. Earlier work by Sroda et al. [11] and Wood et al. [12] has shown that pure metal-ion implantation without deposition can be obtained using a vacuum-arc plasma source. Therefore, a vacuum-arc plasma source offers a good way to introduce metal ions into the materials by metal plasma-immersion ion implantation (MePIII). Recent improvements have been made on our vacuum-arc plasma source that encompasses curved magnetic filters to increase the metal-plasma density and plasma transport efficiency. Pure titanium or tantalum PIII is performed by using longer implantation voltage pulses than cathodic-arc pulses to introduce more metal ions into the surface of the 9Cr18 steel samples. Afterwards, nitrogen plasma-immersion ion implantation is carried out without breaking vacuum. Our results show that the samples implanted with (Ti+N) and (Ta+N) possess better tribological properties than those treated by nitrogen PIII alone.

* Corresponding author. Tel: +852-27887724; fax: +852-27887830/27889549.
E-mail address: paul.chu@cityu.edu.hk (P.K. Chu)

0257-8972/99/$ - see front matter
PII: S0257-8972(99)00178-4

2. Improved vacuum-arc plasma source

In order to increase the plasma transport efficiency of the filter, the duct wall should be biased to a positive voltage [13,14]. However, a positively biased electrode, as introduced by Bilek et al. [15], can achieve the same purpose when placed on the outer section of the curved duct wall (hereafter referred to as 'Bilek bias plate'). In our improved vacuum-arc plasma source, a 90° Bilek bias plate is inserted into the filtering duct. A direct current (DC) voltage is added between the Bilek plate and the ground (arc anode at ground). The bias value is optimized by measuring the metal-ion current on a collecting plate placed in the vacuum chamber with the magnetic field varying between 120 and 560 Gauss and the arc parameters fixed. The experimental results are displayed in Fig. 1. The best results are achieved when the Bilek plate is biased between +10 V and +20 V. A factor of four improvement in the transport efficiency is accomplished at a bias of about +15 V.

To increase the current further, a magnetic coil is installed at the chamber entrance of the plasma source to minimize scattering of the metal plasma. The length of filter duct is also reduced; i.e., the distance traversed by the metal ions is shortened to increase the transport efficiency. A high-capacity power supply is added to produce the higher arc current and longer pulse width in order to enhance the plasma density and efficiency of the vacuum-arc plasma source.

3. Experimental

9Cr18 martensitic stainless steel is widely used as a bearing material, especially in the aerospace industry. Pieces of 9Cr18 bearing steel (composition in wt%: Fe, 79.655; Si, 0.8; Mn, 0.72; P, 0.035; S, 0.03; C, 0.96; Cr, 17.8) were cut from an exterior race of a real industrial bearing which was in the quenched-and-tempered state with a microhardness of about HV560 at the load of 25 g. The samples first received a final polish to a surface roughness (R_a) of 0.04 μm, followed by an ultrasonic clean in acetone. The PIII experiment was carried out in a multi-purpose plasma-immersion ion implanter [16] equipped with several plasma-generating tools, including radio frequency (RF) discharge, hot-filament discharge and a vacuum-arc metal plasma source. Hence, metal PIII and nitrogen PIII could be performed consecutively without breaking vacuum. The improved vacuum-arc plasma source described in the previous section was used to implant titanium and tantalum ions into the 9Cr18 samples. A glow-discharge nitrogen plasma ignited by heated filaments was employed to implant nitrogen into the specimens. Table 1 lists the treatment parameters. Samples #3 to #6 were treated by metal PIII. The arc current, target bias and implantation current measured by an oscilloscope are plotted in Fig. 2. Synchronization of the sample high voltage and arc pulses ensured pure metal plasma-immersion ion implantation without significant metal deposition. After metal PIII, samples #3 to #6 were treated by nitrogen PIII. For comparison, sample #1 and #2 only underwent nitrogen PIII. The experimental conditions of nitrogen PIII are summarized in Table 2.

The coefficient of friction was measured on all the samples using a pin-on-disk wear tester equipped with a ruby ball 3 mm in diameter. The tests were conducted using a load of 50 g and a sliding speed of 1×10^{-3} m s^{-1}. An MXT-α7 digital microhardness tester was operated with a load of 25 g to measure the microhardness of each sample. Chemical analysis of the implanted layers was carried out by X-ray photoelectron spectroscopy (XPS) and elemental depth profiles were acquired by Auger electron spectroscopy (AES) to derive the retained doses.

4. Results and discussion

Fig. 3 displays the microhardness values of the seven samples. The improvement in microhardness after PIII

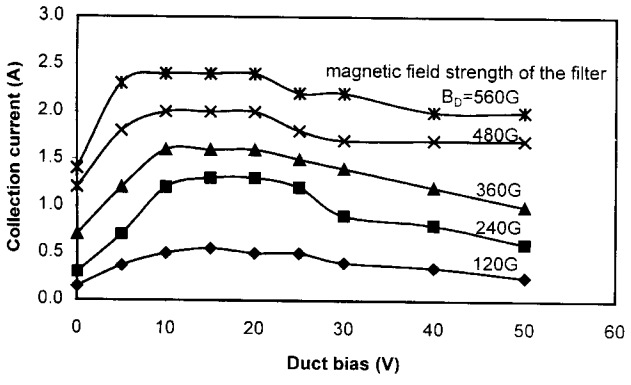

Fig. 1. Collection current as a function of duct bias voltage, with the guiding magnetic field strength as the variable.

Table 1
Experimental parameters of metal PIII using vacuum-arc plasma source

	Sample			
	#3	#4	#5	#6
Cathode material	Ti	Ti	Ta	Ta
Arc peak current (A)	300	300	300	300
Arc pulse duration (μs)	230	230	230	230
Implantation voltage (kV)	25	25	25	25
Implantation pulse width (μs)	280	280	280	280
Pulse repetition rate (Hz)	33	33	33	33
Base pressure (Pa)	3×10^{-3}	3×10^{-3}	3×10^{-3}	3×10^{-3}
Implantation time (min)	80	80	80	80

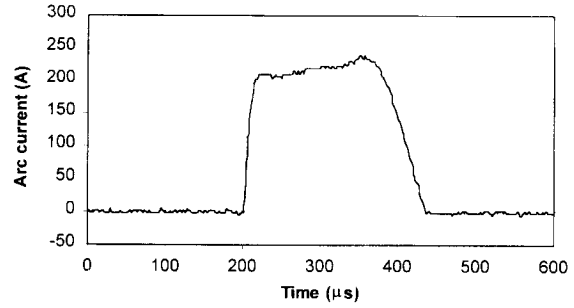

(a)

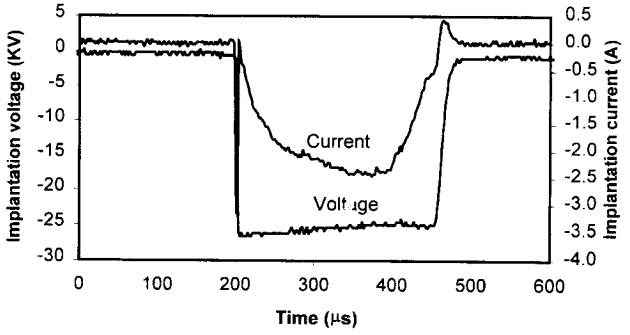

(b)

Fig. 2. Oscilloscope traces of (a) arc current, and (b) implantation voltage pulse and implantation current, during metal plasma-immersion ion implantation.

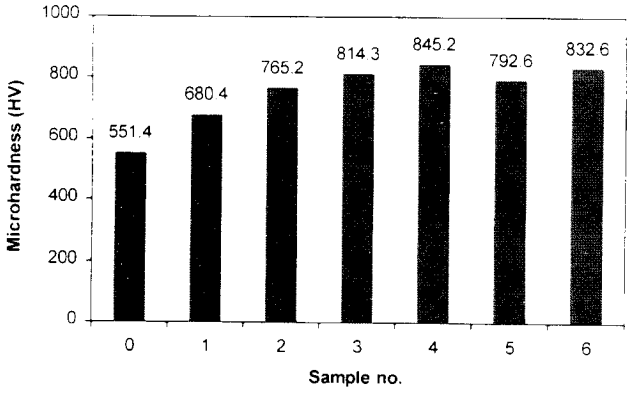

Fig. 3. Microhardness of the seven 9Cr18 samples.

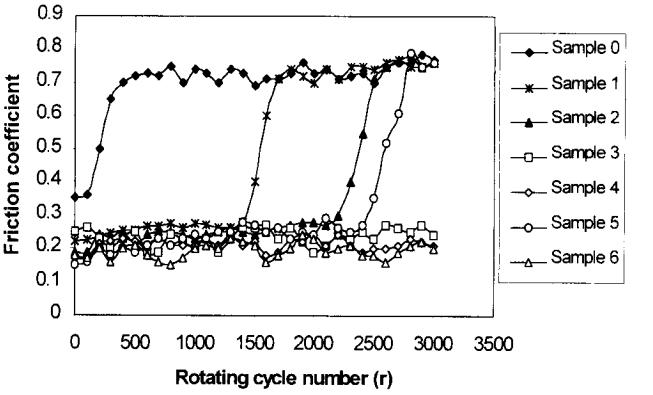

Fig. 4. Coefficient of friction curves of the 9Cr18 samples.

treatment under various conditions is evident, with the maximum increase in hardness being 53%. The samples implanted with metal plus nitrogen ions (samples #3 to #6) have higher microhardness than the samples treated by nitrogen PIII only. This indicates that implanting titanium or tantalum into 9Cr18 steel yields a harder surface layer. A higher nitrogen implantation dose (i.e., comparing samples #1 and #2) can also enhance the microhardness of 9Cr18 materials.

The samples were subjected to a friction test of 3000 cycles. The coefficient of friction was measured during the test, and the wear tracks were inspected under an optical microscope to determine the track width after the test. A comparison of the seven samples is displayed in Fig. 4. The unimplanted sample has a relatively high coefficient of friction (0.7–0.8) and, at the beginning of the test, the value is lower due to the existence of a small amount of water and adsorbates on the surface. As this layer is broken during the test, the coefficient of friction increases rapidly after about 100 cycles. In comparison, for samples #1 to #6, the coefficient of friction starts at a lower value (0.1–0.3) and maintains this level as a result of the modified layer on the surface. With increasing rotating cycles, the coefficient of friction of three of the samples (#1, #2 and #5) eventually reaches the same value (0.7–0.8) as that of the unimplanted sample. This is because the implanted layer is damaged and the underlying substrate is exposed.

Table 2
Experimental conditions of nitrogen PIII

	Sample						
	#0	#1	#2	#3	#4	#5	#6
Implantation bias voltage (kV)	none	35	35	35	35	35	35
Pulse width (μs)		30	30	30	30	30	30
Pulse repetition rate (Hz)		300	300	300	300	300	300
Discharge voltage (V)		80	80	80	80	80	80
Discharge current (A)		1	1	1	1	1	1
Gas pressure (Pa)		2×10^{-2}	2×10^{-2}	2×10^{-2}	2×10^{-2}	2×10^{-2}	2×10^{-2}
Implantation time (h)	untreated	2	4	2	4	2	4

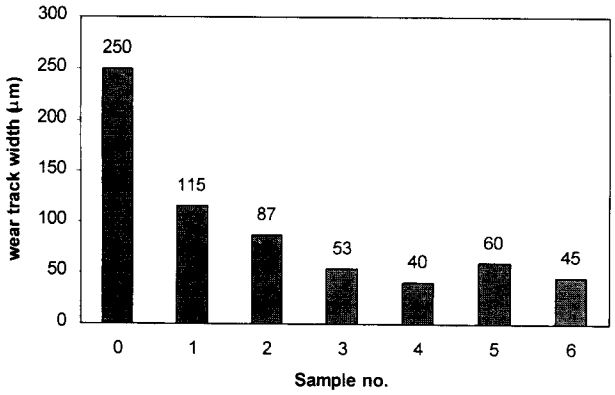

Fig. 5. Wear track width of the seven 9Cr18 samples.

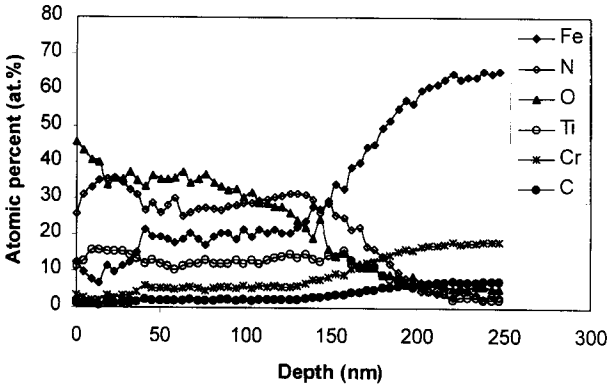

Fig. 6. AES depth profiles acquired from sample #4.

For samples #3, #4 and #6, the coefficient of friction remains small throughout the test. This implies that the surface-modified layers in these three samples have not been broken even after 3000 rotating cycles, and they have a highly wear-resisting layer on the surface. It can be observed that the samples implanted with (Ti+N) have better tribological properties. Fig. 5 depicts the wear track width of each sample after a pin-on-disk wear test of 3000 rotating cycles. The results are similar to those of the friction test. The PIII samples have smaller track widths than the unimplanted sample. In addition, the samples treated by metal plus nitrogen PIII have smaller track widths than that the samples treated by nitrogen PIII alone.

Fig. 6 shows the elemental depth profiles acquired from sample #4 by Auger electron spectroscopy. The thickness of the modified layer is about 240 nm; this is larger than the computed projected ranges of the implanted ions, thereby confirming in situ diffusion of nitrogen and titanium atoms. The calculated retained doses of titanium and nitrogen are 2.92×10^{17} atoms cm^{-2} and 5.7×10^{17} atoms cm^{-2}, respectively. Coupled with the tribological test results, it can be inferred that the coexistence of titanium or tanatalum with nitrogen plays a key role in improving the surface properties of 9Cr18 steel.

Fig. 7 shows the N 1s XPS spectra acquired from samples #3 and #5 at various depths. The sputtering rate was 40 Å min^{-1} and the energy spectra were acquired at three depths: surface, 200 Å and 600 Å. Sample #3 shows only one salient peak at 400 eV on the surface. This peak corresponds to the α' martensite containing nitrogen and α'' phase ($Fe_{16}N_2$). After sputtering for 5 min (i.e., at a depth of 200 Å), two peaks appear. The peak at 400 eV becomes smaller while the 396.5 eV peak becomes more dominant. The latter peak corresponds to the nitride state and is close to the binding energy of Cr_2N, CrN and TiN. Therefore, many nitride phases have formed at a depth of 200 Å. After sputtering for 15 min (i.e., at a depth of 600 Å), the peak at 400 eV almost disappears illustrating that, at

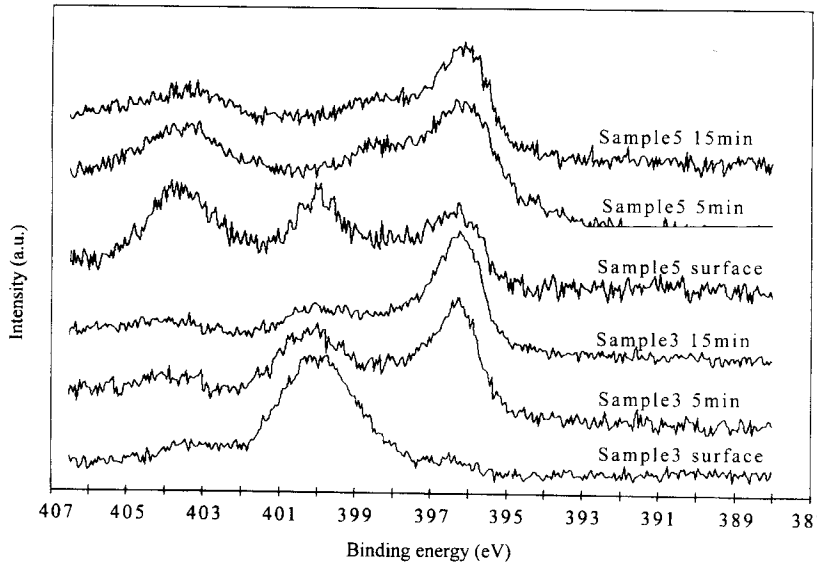

Fig. 7. N 1s XPS spectra of samples #3 and #5 at different depths.

this depth, the implanted nitrogen atoms exist exclusively as nitrides. Nitride phases are known to have very high hardness and are believed to give rise to the superior microhardness and tribological properties reported in this work. The spectra acquired from sample #5 show a similar trend except that the surface spectrum shows three peaks at 403 eV, 400 eV and 396.5 eV. The peak at 403 eV shows the formation of metallic nitric oxide (Me_3NO) stemming from minute oxygen contamination in the vacuum chamber. The peak at 396.5 eV indicates that nitride phases have formed on the surface of sample #5. The 403 eV peak diminishes with increasing sputtering depth. After sputtering for 15 min, this peak almost disappears as the amount of oxygen decreases. After sputtering for 5 min, the 400 eV peak no longer exists. The implanted nitrogen atoms mainly exist as nitrides as demonstrated by the fact that the 396.5 eV peak is the dominant one. After sputtering for 15 min, there is only one peak which corresponds to nitrides such as Cr_2N, CrN and TaN, implying that nitrides have become the dominant chemical state of nitrogen at this depth. These nitride phases with superior hardness exist in a dispersed state in the implanted layer and result in a dispersed phase hardening. They are believed to be responsible for the improvement in both the microhardness and wear properties.

5. Conclusion

The microhardness and wear properties of 9Cr18 bearing steel are improved significantly by using plasma-immersion ion implantation. Sequential metal and nitrogen PIII is an efficient method to introduce multiple elements into steels. Our experimental results indicate that the tribological properties of the samples implanted with (Ti+N) and (Ta+N) are enhanced to a larger degree than those of samples treated by nitrogen PIII alone. The XPS data show nitrides in the implanted layer, and these are believed to play a key role in the improvement of the tribological properties of 9Cr18 steel. Our results confirm the efficiency of the improved metal-arc source and show that metal and nitrogen PIII is an effective way to enhance the microhardness, wear properties and lifetime of 9Cr18 bearing steel.

Acknowledgements

The work was supported by Hong Kong Research Grants Council Earmarked Grants 9040332 and 9040344, as well as by City University of Hong Kong Strategic Research Grant #7000964.

References

[1] J.C. Jin, C.G. Zhao, Grinding Affected Layer andSurface Modification, Hunan University Press, People's Republic of China, 1992, p. 1.
[2] Y.R. Wang, J. Chen, Aerospace Manuf. Eng. 5 (1993) 16.
[3] J.R. Conrad, S. Baumann, R. Fleming, G.P. Meeker, J. Appl. Phys. 65 (4) (1989) 1701.
[4] A. Chen, J.T. Scheure, C. Ritter, R.B. Alexander, J.R. Conrad, J. Appl. Phys. 70 (11) (1991) 6757.
[5] G.A. Collins, R. Hutchings, J. Tendys, M. Samandi, Surf. Coat. Technol. 68 (1994) 285.
[6] S.Y. Wang, P.K. Chu, B.Y. Tang, X.C. Zeng, Y.B. Chen, X.F. Wang, Surf. Coat. Technol. 93 (1997) 309.
[7] S.Y. Wang, P.K. Chu, B.Y. Tang, X.C. Zeng, X.F. Wang, Nucl. Instrum. Methods B 127 (1997) 100.
[8] J.W. Mayer, L. Eriksson, J.A. Davies, Ion Implantation in Semiconductors, Academic Press, New York, 1971, p. 2.
[9] A. Anders, Surf. Coat. Technol. 93 (1997) 158.
[10] A. Anders, S. Anders, I.G. Brown, M.R. Dickinson, R.A. MacGill, J. Vac. Sci. Technol. B 12 (2) (1994) 815.
[11] T. Sroda, S. Meassick, C. Chan, Appl. Phys. Lett. 60 (9) (1992) 1076.
[12] B.P. Wood, W.A. Reass, I. Henins, Surf. Coat. Technol. 85 (1996) 70.
[13] I.I. Aksenov, V.A. Belous, V.G. Padalka, V.M. Khoroshikh, Instrum. Exp. Tech. 21 (1978) 1416.
[14] A. Anders, S. Anders, I.G. Brown, J. Appl. Phys. 75 (1994) 4900.
[15] M.M.M. Bilek, D.R. McKenzie, Y. Yin, M. Chowalla, W.I. Milne, IEEE Trans. Plasma Sci. 24 (5) (1996) 1291.
[16] P.K. Chu, B.Y. Tang, Y.C. Cheng, P.K. Ko, Rev. Sci. Instrum. 68 (4) (1997) 1866.